Biogeosciences Discuss., doi:10.5194/bg-2016-66, 2016
Manuscript under review for journal Biogeosciences
Published: 29 February 2016

Ocean acidification in the North Atlantic: controlling mechanisms

Maribel I. García-Ibáñez[1], Patricia Zunino[2], Friederike Fröb[3], Lidia I. Carracedo[4], Aida F. Ríos[†], Herlé Mercier[5], Are Olsen[3], Fiz F. Pérez[1]

[1]Instituto de Investigaciones Marinas, IIM-CSIC, Vigo, E36208, Spain.
[2]Ifremer, Laboratoire de Physique des Océans, UMR 6523 CNRS/Ifremer/IRD/UBO, Ifremer Centre de Brest, Plouzané, CS 10070, France.
[3]Geophysical Institute, University of Bergen and Bjerknes Centre for Climate Research, Bergen, N5007, Norway.
[4]Faculty of Marine Sciences, University of Vigo, Vigo, E36200, Spain.
[5]CNRS, Laboratoire de Physique des Océans, UMR 6523 CNRS/Ifremer/IRD/UBO, Ifremer Centre de Brest, Plouzané, CS 10070, France.
[†]Deceased.

Correspondence to: Maribel I. García-Ibáñez (maribelgarcia@iim.csic.es)

Abstract. Repeated hydrographic sections provide critically needed data on, and understanding of, changes in basin-wide ocean CO_2 chemistry over multi-decadal timescales. Here, high-quality measurements collected at thirteen cruises carried out along the same track between 1981 and 2015, have been used to determine long-term changes in ocean CO_2 chemistry and ocean acidification in the Irminger and Iceland basins of the North Atlantic Ocean. Trends were determined for each of the main water masses present and are discussed in the context of the basin-wide circulation. The pH has decreased in all water masses of the Irminger and Iceland basins over the past 34 years, with the greatest changes in surface and intermediate waters (between -0.0008 ± 0.0001 pH units·yr^{-1} and -0.0013 ± 0.0001 pH units·yr^{-1}). In order to disentangle the drivers of the pH changes, we decomposed the trends into their principal drivers: changes in temperature, salinity, total alkalinity (A_T) and total dissolved inorganic carbon (both its natural and anthropogenic components). The increase of anthropogenic CO_2 (C_{ant}) was identified as the main agent of the pH decline, partially offset by A_T increases. The acidification of intermediate waters caused by C_{ant} uptake has been reinforced by the aging of the water masses over the period of our analysis. The pH decrease of the deep overflow waters of the Irminger basin was similar to that observed in the upper ocean, and was mainly linked to the C_{ant} increase, thus reflecting the recent contact of these deep waters with the atmosphere.

Keywords. Ocean acidification; C_{ant}; water masses; Subpolar Gyre.

1 INTRODUCTION

The oceanic uptake of a fraction of the anthropogenic CO_2 (i.e., C_{ant}; CO_2 released from humankind's industrial and agricultural activities) has resulted in long-term changes in ocean CO_2 chemistry, commonly referred to as ocean acidification, OA (e.g., Caldeira and Wickett, 2003, 2005; Raven et al., 2005; Doney et al., 2009; Feely et al., 2009). The changes in the ocean CO_2 chemistry result in declining pH and reduced saturation states for $CaCO_3$ minerals (e.g., Bates et al., 2014). The average pH ($-\log_{10}[H^+]$) of ocean surface waters has decreased by about 0.1 pH units since the beginning of the industrial revolution (1750), and based on model projections we expect an additional drop of 0.1–0.4 by the end of this century, even under conservative CO_2 emission scenarios (Caldeira and Wickett, 2005; Orr, 2011; Ciais et al., 2013). The rate of change in pH is at

Biogeosciences Discuss., doi:10.5194/bg-2016-66, 2016
Manuscript under review for journal Biogeosciences
Published: 29 February 2016

least a hundred times faster than at any time since the last Ice Age (Feely et al., 2004; Raven et al., 2005), clearly outpacing natural processes in ocean chemistry that have occurred in the past due to geological processes (Raven et al., 2005). These changes in ocean CO_2 chemistry will most likely have adverse effects on organisms, particularly calcifying ones, on ecosystems (e.g., Langdon et al., 2000; Riebesell et al., 2000; Pörtner et al., 2004; Orr et al., 2005; Doney et al., 2009; Gattuso et al., 2014) and on major marine biogeochemical cycles (e.g., Gehlen et al., 2011; Matear and Lenton, 2014).

The global ocean has absorbed ~30% of the C_{ant} emitted to the atmosphere between 1750 and the present (Sabine et al., 2004; Khatiwala et al., 2013; DeVries, 2014; Le Quéré et al., 2015). This C_{ant} is not evenly distributed throughout the oceans (Sabine et al., 2004), but enters the interior ocean preferentially in regions of deep convective overturn and subduction (Maier-Reimer and Hasselmann, 1987; Sarmiento et al., 1992; Lazier et al., 2002). This explains why the Meridional Overturning Circulation (MOC) makes the North Atlantic Ocean one of the most important C_{ant} sinks of the global ocean, storing 25% of the global oceanic C_{ant} (Sabine et al., 2004; Khatiwala et al., 2013) despite being only 11% of the global ocean volume (Eakins and Sharman, 2010). The MOC transports C_{ant}-laden surface waters from the Equator to the northern North Atlantic Ocean (e.g., Wallace, 2001; Anderson and Olsen, 2002; Álvarez et al., 2003; Olsen et al., 2006; Quay et al., 2007; Zunino et al., 2015b), where deep water formation provides a pathway for C_{ant} into the interior ocean (Lazier et al., 2002; Pérez et al., 2008; Steinfeldt et al., 2009; Pérez et al., 2013). As regions close to deep water formation areas and where water mass transformation occurs (Sarafanov et al., 2012; García-Ibáñez et al., 2015), the Irminger and Iceland basins are geographically well placed to monitor temporal changes in the Atlantic MOC (Mercier et al., 2015), and to determine the rates of C_{ant} penetration to the deep ocean and its consequence for OA.

In this paper, we examine high-quality direct measurements of ocean CO_2 chemistry taken from thirteen cruises conducted across the Irminger and Iceland basins between 1981 and 2015. Previous studies focused on the C_{ant} uptake and its storage and effect on pH in the Irminger and Iceland basins (e.g., Pérez et al., 2008; Olafsson et al., 2009; Bates et al., 2012; Vázquez-Rodríguez et al., 2012b). Here we quantify OA for an extended period and identify its chemical and physical drivers, based on direct measurements.

2 MATERIALS and METHODS

2.1 Datasets

2.2.1 Cruise Information

We used thirteen cruises along the same track across the Irminger and Iceland basins, with the cruise dates spanning 34 years (1981–2015; Table 1, Fig. 1a). The bottle data were accessed from the merged data product of the Global Data Analysis Project version 2 (GLODAPv2; Olsen et al., 2016) at http://cdiac.ornl.gov/oceans/GLODAPv2, except for more recent unpublished data collected during the OVIDE 2012 and 2014 cruises and the 2015 cruise (58GS20150410). The data of the 1991 cruises (64TR91_1 and 06MT18_1) were merged and treated as a single cruise.

2.2.2 Ocean CO_2 chemistry measurements

At least two variables of the seawater CO_2 system were measured on all cruises included in our analyses, but the measured pairs varied between cruises. The total alkalinity (A_T) was analysed by potentiometric titration and

Biogeosciences Discuss., doi:10.5194/bg-2016-66, 2016
Manuscript under review for journal Biogeosciences
Published: 29 February 2016

determined by developing either a full titration curve (Millero et al., 1993; Dickson and Goyet, 1994; Ono et al., 1998) or from single point titration (Pérez and Fraga, 1987; Mintrop et al., 2000), with an overall accuracy of 4 $\mu mol \cdot kg^{-1}$. For samples without direct A_T measurements, it was estimated using a 3D moving window multilinear regression algorithm (3DwMLR), using potential temperature (θ), salinity, nitrate, phosphate, silicate and oxygen as predictor parameters (Velo et al., 2013). The total dissolved inorganic carbon (DIC) samples were analysed with coulometric titration techniques (Johnson et al., 1993), and were calibrated with Certified Reference Materials (CRMs), achieving an overall accuracy of 2 $\mu mol \cdot kg^{-1}$. The exception to the use of this analytical technique was the 1981 TTO-NAS (Transient Tracer in the Ocean-North Atlantic Survey) cruise, where DIC was determined potentiometrically (Bradshaw et al., 1981) and no CRMs were used. The TTO-NAS DIC measurements were deemed unreliable (Brewer et al., 1986), therefore, the DIC values compiled in the GLODAPv2 merged data product are those calculated from pCO_2 and revised A_T reported by Tanhua and Wallace (2005). pH was determined either potentiometrically (Dickson, 1993a, b) using pH electrodes or, more commonly, with a spectrophotometric method (Clayton and Byrne, 1993) using either scanning or diode array spectrophotometers and m-cresol purple as an indicator. The spectrophotometric pH determination has a typical precision of 0.0002–0.0004 pH units (Clayton and Byrne, 1993; Liu et al., 2011). However, Carter et al. (2013) reported an inaccuracy of the spectrophotometric pH determination of 0.0055 pH units. When direct pH measurements were not performed, it was computed from A_T and DIC using the thermodynamic equations of the seawater CO_2 system (Dickson et al., 2007) and the CO_2 dissociation constants of Mehrbach et al. (1973) refitted by Dickson and Millero (1987). For these calculated pH values, we estimated an uncertainty of 0.006 pH units by random propagation of the reported A_T and DIC accuracies. The exception to the latter is the 1981 TTO-NAS cruise, whose DIC problems caused the estimated uncertainty for calculated pH values to be slightly higher (0.008 pH units). A_T data from the 1981 TTO-NAS cruise were checked against A_T values generated by the 3DwMLR (Velo et al., 2013). A_T values differing by more than two times the standard deviation (confidence interval; 7 $\mu mol \cdot kg^{-1}$) of the difference between measured A_T and 3DwMLR predicted A_T were replaced with the predicted A_T value. However, for leg 6 of the 1981 TTO-NAS cruise (which was not analysed by Tanhua and Wallace (2005)) the limit of substitution for the predicted A_T value was lowered to 4 $\mu mol \cdot kg^{-1}$. Note that the effect of A_T corrections on pH trends is negligible, since A_T corrections of 4 $\mu mol \cdot kg^{-1}$ lead to pH changes lower than a thousandth. The pH values reported here are at in situ conditions and on the total scale (pH_{Tis}).

2.2.3 Anthropogenic CO_2 (i.e., C_{ant}) estimation

C_{ant} concentrations were estimated using the back-calculation method φC_T^0 (Pérez et al., 2008; Vázquez-Rodríguez, 2009a) that has previously been applied for the entire Atlantic Ocean (Vázquez-Rodríguez et al., 2009b). Back-calculation methods determine C_{ant} for any sample in the water column as the difference between DIC concentration at the time of the measurement and the DIC concentration it would have had in preindustrial times. This is represented as the difference in preformed DIC between the time of observation and the preindustrial as:

$$C_{ant} = DIC_{meas} - \Delta C_{bio} - DIC_{preind} - \Delta C_{diseq}, \quad (1)$$

where the preformed DIC for the time of observation is represented as the measured DIC (DIC_{meas}) less any DIC added to the water due to organic matter remineralisation and calcium carbonate dissolution (ΔC_{bio}), and the preindustrial preformed concentration is represented by the DIC concentration the water would have if in

Biogeosciences Discuss., doi:10.5194/bg-2016-66, 2016
Manuscript under review for journal Biogeosciences
Published: 29 February 2016

equilibrium with the preindustrial atmosphere (DIC_{preind}) less any offset from such an equilibrium value, known as the disequilibrium term (ΔC_{diseq}). The procedure requires DIC and A_T as input parameters, and the empirical parameterization of the preformed A_T (A_T^0) for the computation of the calcium carbonate dissolution and of the ΔC_{diseq} term.

The φC_T^0 method presents two main advantages. First, the spatiotemporal variability of A_T^0 is taken into account. And second, C_{ant} estimation needs no "zero-C_{ant}" reference, since the parameterizations of A_T^0 and ΔC_{diseq} are determined using the subsurface layer as reference for water mass formation conditions (Vázquez-Rodríguez et al., 2012a). The overall uncertainty of the method has been estimated at 5.2 μmol·kg^{-1} (Pérez et al., 2008; Vázquez-Rodríguez, 2009a).

The reproducibilities and uncertainties of the main variables were determined from the deep waters sampled at Iberian Abyssal Plain during the seven repeats of the OVIDE line, since these waters are expected to be in near-steady state. The confidence intervals of those samples for each cruise (Table 2) were taken as an estimate of the uncertainty of the methodologies. The uncertainties of the Apparent Oxygen Utilization (AOU; the difference between the saturated concentrations of oxygen calculated using the equations of Benson and Krause (1984) and the measured concentrations of oxygen), A_T and pH on the total scale at 25ºC (pH_{T25}) for the seven cruises were similar. The confidence intervals of C_{ant} (2.4–3.2 μmol·kg^{-1}) and pH_{T25} (0.004–0.006 pH units) across the seven cruises are lower than the inherent uncertainty of the φC_T^0 estimates (5.2 μmol·kg^{-1}) and the accuracy of the spectrophotometric pH measurements (0.0055 pH units), which provides confidence that these data are suitable for trend determination. The confidence intervals of the C_{ant} estimates are rather similar than in other regions where C_{ant} has been compared across many cruises (i.e., 2.4 μmol·kg^{-1} in the South Atlantic Ocean, Ríos et al. (2003); 2.7 μmol·kg^{-1} in the Equatorial Atlantic Ocean, 24ºN, Guallart et al. (2015); and 2.7 μmol·kg^{-1} reported from a transect along the western boundary of the Atlantic Ocean from 50ºS to 36ºN, Ríos et al. (2015)). The confidence interval of the mean values of the Iberian Abyssal Plain samples across the seven cruises (last row of Table 2) was taken as an estimate of the reproducibility of the methodologies. The high reproducibilities, an order of magnitude lower than the uncertainties, render confidence to the estimated trends.

2.2 Water mass characterization

Changes in ocean CO_2 chemistry were determined for the main water masses in the Irminger and Iceland basins. These are: (1) Subpolar Mode Water (SPMW); (2) upper and classical Labrador Sea Water (uLSW and cLSW, respectively); (3) Iceland–Scotland Overflow Water (ISOW) and; (4) Denmark Strait Overflow Water (DSOW; Fig. 1b). The layers defining the water masses were delimited using potential density following Azetsu-Scott et al. (2003), Kieke et al. (2007), Pérez et al. (2008) and Yashayaev et al. (2008).

To better determine the interfaces between layers and the average value of each variable in each layer, cruise bottle data were linearly interpolated onto each dbar before determining average variable values, an improvement with respect to the previous approaches of Pérez et al. (2008, 2010) and Vázquez-Rodríguez et al. (2012b). Upper layer data (pressure ≤ 100 dbar) were replaced with the mean value in the pressure range 50–100 dbar to reduce the influence of seasonal differences in sampling on the inter-annual trends (Vázquez-Rodríguez et al., 2012a). Then, the interpolated profiles were divided into the different water mass density intervals (Fig. 1b). Next, the variables were averaged over each density layer on a station by station basis for each cruise. Finally, the average values in each density layer were determined for each cruise taking into account the

Biogeosciences Discuss., doi:10.5194/bg-2016-66, 2016
Manuscript under review for journal Biogeosciences
Published: 29 February 2016

thickness of the layer and the separation between stations. Note that average values of pressure sensitive parameters, i.e. pH_{Tis}, were referred to the mean pressure of the layer over the studied time period to avoid the effects of the heaving of the water masses due to warming and/or of the sampling strategy over the pH trends. The average values of the variables for each layer and their confidence intervals can be found in the Supplementary Table S1.

2.3 pH deconvolution

Changes in ocean pH may be brought about by changes in in situ temperature (T_{is}), salinity (S), A_T, and/or DIC, of which changes in the latter may be brought about by C_{ant} uptake or by natural processes (C_{nat}), such as remineralisation. C_{nat} is determined as the difference between measured DIC and estimated C_{ant}. To estimate how much each of these altogether five factors contributed to the observed change in pH, we assumed linearity and decomposed the observed pH changes into these potential drivers according to:

$$\frac{dpH_{Tis}}{dt} = \frac{\partial pH_{Tis}}{\partial T_{is}}\frac{dT_{is}}{dt} + \frac{\partial pH_{Tis}}{\partial S}\frac{dS}{dt} + \frac{\partial pH_{Tis}}{\partial A_T}\frac{dA_T}{dt} + \frac{\partial pH_{Tis}}{\partial DIC}\frac{d(C_{nat}+C_{ant})}{dt}, \quad (2)$$

To estimate $\frac{\partial pH_{Tis}}{\partial var}$ (where var refers to each of the drivers: T_{is}, S, A_T and DIC) we calculated the mean pH_{Tis} for each layer and cruise using the real average value of var but keeping the values of the other three drivers constant and equal to the mean value for the layer over all the cruises. To estimate each $\frac{\partial var}{\partial t}$ term we performed a linear regression between var and time for each layer.

Trends of all variables involved in Eq. (2) were calculated using the annual interpolation of the observed values to avoid the bias due to the reduced availability of cruises during the 80's and 90's with respect to the 2000's.

3 RESULTS AND DISCUSSION

3.1 Mean distribution of water mass properties

The Irminger and Iceland basins in the North Atlantic are characterized by warm and saline surface waters, and cold and less saline intermediate and deep waters (Fig. 2a,b). The central waters (here represented by the SPMW layer), which dominates the upper ~700 m, are warmer and saltier in the Iceland basin than in the Irminger basin, reflecting the water mass transformation that takes place along the path of the North Atlantic Current (NAC) (Brambilla and Talley, 2008). In particular, the mixing of the SPMW layer with the surrounding waters while flowing around the Reykjanes Ridge (evident in the salinity distribution; see also García-Ibáñez et al. (2015)), in conjunction with the air−sea heat loss, results in a colder and fresher SPMW layer in the Irminger basin. The uLSW and cLSW layers, below the SPMW layer, are warmer and saltier in the Iceland basin due to their mixing with the surrounding waters during their journey from their formation regions (Bersch et al., 1999; Pickart et al., 2003; García-Ibáñez et al., 2015). The ISOW layer dominates at depths beneath the cLSW layer. This layer is warmer and saltier in the Iceland basin, reflecting its circulation. ISOW comes from the Iceland–Scotland sill and flows southwards into the Iceland basin, where it mixes with the older North Atlantic Deep Water (NADW). Then, it crosses the Reykjanes Ridge through the Charlie−Gibbs Fracture Zone (Fig. 1a), where it mixes with the recently ventilated cLSW and DSOW, becoming colder and fresher. In the bottom of the Irminger basin, a fifth layer is distinguished, DSOW, being the coldest and freshest layer of the section.

Biogeosciences Discuss., doi:10.5194/bg-2016-66, 2016
Manuscript under review for journal Biogeosciences
Published: 29 February 2016

The general pattern of pH_{Tis} (Fig. 2c) follows by and large the distribution expected from the surface production of organic material and remineralisation at depth. The high surface values (> 8.05) are the result of the withdrawing of DIC by photosynthetic activity, while the values generally decrease with depth down to < 7.95 in the deepest layers, because of the DIC concentration increase resulting from remineralisation. This overall pattern is disrupted at ~500 m in the Iceland basin by a layer with relatively low pH_{Tis} values (< 7.98), coinciding with relatively high AOU and DIC values (Fig. 2e,f). This layer could be associated to an area of slower circulation where the products of the remineralization of the organic matter accumulate. This thermocline layer could also been influenced by waters of southern origin (Sarafanov et al., 2008), which are advected into the region by the NAC, whose arrival is closely related with the North Atlantic Oscillation (Desbruyères et al., 2013). The presence of this low pH layer lowers the average pH of our SPMW layer in the Iceland basin compared to the Irminger basin (Fig. 3). An opposite pattern is found in the uLSW layer. The water mass formation occurring in the Irminger basin (Pickart et al., 2003; García-Ibáñez et al., 2015; Fröb et al., 2016; Piron et al., 2016) transfers recently ventilated low DIC and high pH waters to depth, which causes the mean pH of uLSW in the Irminger basin to be higher than in the Iceland basin. Finally, the layers that contain the overflow waters have the lowest pH values. The presence of the older NADW in the ISOW layer in the Iceland basin decreases the mean pH of this layer here, making it lower than in the Irminger basin.

The surface waters of the section have low DIC values, which rapidly increase when increasing depth (Fig. 2f). The low DIC values in the uppermost ~200 m are also related to the photosynthetic activity that withdraws DIC from seawater. Below ~200 m the DIC distribution is almost homogeneous, only disrupted by relatively high values in the Iceland basin at ~500 m associated with the thermocline layer, and at the bottom, associated with the old NADW. The gradients in DIC anthropogenic and natural components are much stronger. This is because the C_{ant} and C_{nat} distributions are anti-correlated. The C_{ant} values are high, close to saturation (80% of saturation), near the surface and decrease with depth (Fig. 2h), because Cant enters the ocean from the atmosphere. The C_{nat} distribution has an opposite pattern, similar to that of the AOU distribution (Fig. 2e), with low surface values and high bottom values (Fig. 2g), for reasons discussed above.

The A_T distribution along the section resembles the salinity distribution, with high values associated with the relatively saline central waters and low and almost homogeneous values in the rest of the section (Fig. 2d). The exception comes with the deep waters of the Iceland basin, which have among the highest A_T values while salinity is not extraordinarily high. This reflects the influence of NADW, which contains relatively large amounts of silicate related to the influence of the Antarctic Bottom Water.

3.2 Water mass acidification and drivers

Trends of pH_{Tis} in each layer and basin are presented in Table 3 and Fig. 3. The pH_{Tis} has decreased in all layers of the Irminger and Iceland basins during the time period of more than 30 years (1981–2015) that is covered by our data. The trends are stronger in the Irminger basin due to the presence of younger waters. The rate of OA decreases with depth, except for the DSOW layer that has acidification rates close to those found in the cLSW layer. This indicates that DSOW is a newly formed water that has recently been in contact with the atmosphere. Moreover, the acidification rate in the ISOW layer in the Irminger basin is relatively low, which could be related to the increasing importance on this layer of the relatively old NADW with the diminution in volume of cLSW since mid-90s (Lazier et al., 2002; Yashayaev, 2007).

Biogeosciences Discuss., doi:10.5194/bg-2016-66, 2016
Manuscript under review for journal Biogeosciences
Published: 29 February 2016

The observed rate of pH_{Tis} decrease in the SPMW layer of the Iceland basin (-0.0012 ± 0.0001 pH units·yr^{-1}; Table 3, Fig. 3b) is in agreement with that observed at the Iceland Sea time-series (68ºN, 12.66ºW; Olafsson et al. (2009, 2010)) for the period 1983–2014 (-0.0014 ± 0.0005 pH units yr^{-1}; Bates et al. (2014)). Our rates in the SPMW layer of both basins are slightly lower than those observed at the Subtropical Atlantic time-series stations ESTOC (29.04ºN, 15.50ºW; Santana-Casiano et al. (2007), González-Dávila et al. (2010)) for the period 1995–2014 (-0.0018 ± 0.0002 pH units·yr^{-1}; Bates et al. (2014)) and BATS (32ºN, 64ºW; Bates et al. (2014)) for the period 1983–2014 (-0.0017 ± 0.0001 pH units·yr^{-1}; Bates et al. (2014)). However, our rate of pH_{Tis} decrease in the SPMW layer in the Irminger basin (-0.0013 ± 0.0001 pH units·yr^{-1}) is only half of that observed in the sea surface waters of the Irminger Sea time-series (64.3ºN, 28ºW; Olafsson et al. (2010)) for the period 1983–2014 (-0.0026 ± 0.0006 pH units yr^{-1}; Bates et al. (2014)), which is exceptionally high compared to the other time series summarized here. Comparing with the Pacific Ocean, the OA rates in the Iceland and Irminger basins are slightly lower than those reported for the Central North Pacific based on data from the time-series station HOT (22.45ºN, 158ºW; Dore et al. (2009)) for the period 1988–2014 (-0.0016 ± 0.0001 pH units·yr^{-1}; Bates et al. (2014)), but are in agreement with those found by Wakita et al. (2013) in the winter mixed layer at the Subarctic Western North Pacific (time-series stations K2 and KNOT) for the period 1997–2011 (-0.0010 ± 0.0004 pH units·yr^{-1}).

Vázquez-Rodríguez et al. (2012b) have previously studied the pH changes in the different water masses of the Irminger and Iceland basins. These authors carried out a pH normalization to avoid potential biases due to different ventilation stages and rates of each layer, from the different spatial coverage of the evaluated cruises. The normalized pH values (pH_N) for each layer was obtained using multiple linear regressions between the observed mean pH_{SWS25} (pH at seawater scale and 25ºC) and the observed mean values of θ, salinity, silicate and AOU, referred to the mean climatological values of θ, salinity, silicate and AOU compiled in WOA05 (http://www.nodc.noaa.gov/OC5/WOA05/pr_woa05.html). This normalization, combined with the lower temporal coverage (1981–2008) and the fact that they evaluated trends in pH at 25ºC and not at in situ conditions renders direct comparisons between their and our derived trends difficult.

To infer the causes of the acidification trends reported here, we decomposed the pH trends into their individual components as described in Sect. 2.2. The results are presented in Table 3. The sum of the pH changes caused by the individual drivers (in situ temperature, salinity, A_T and DIC) matches the observed pH trends, which renders confidence to the method.

The temperature changes (Fig. 4a,b) have generally resulted in small to negligible pH declines (Table 3). Specifically, warming corresponds to a pH decrease of more than 0.0001 pH units·yr^{-1} in the SPMW layer of both basins and in the LSW layers of the Irminger basin, while the effect of temperature changes on pH in the other layers is negligible. Temperature driven pH change is larger in the LSW layers in the Irminger than in the Iceland basin. In the case of the uLSW layer, this is possibly explained by the deep convection occurring in the Irminger basin (Pickart et al., 2003; García-Ibáñez et al., 2015; Fröb et al., 2016; Piron et al., 2016). In the case of the cLSW layer, the higher pH changes driven by temperature changes in the Irminger basin could be explained by the rapid advection of this water mass from the Labrador Sea to this basin (Yashayaev et al., 2007). The temperature effect on pH evaluated here is mostly thermodynamic. The same applies to the salinity effect, which however is small to negligible, reflecting that salinity changes in the region (Fig. 4c,d) are insufficiently large to significantly change pH.

Biogeosciences Discuss., doi:10.5194/bg-2016-66, 2016
Manuscript under review for journal Biogeosciences
Published: 29 February 2016

The A_T has increased in all layers (Fig. 5a,b), corresponding to increasing pH (Table 3), which counteracts the acidification from the CO_2 absorption. The contribution from A_T to reduce ocean acidification is significant for all the layers, except for ISOW of the Irminger basin and uLSW of the Iceland basin (in which A_T trends over time are not significant; Fig. 5a,b). The A_T increasing trends observed in SPMW may indicate the increasing presence of waters of subtropical origin (with higher A_T) as the subpolar gyre was shrinking since mid-90s (e.g., Flatau et al., 2003; Häkkinen and Rhines, 2004; Böning et al., 2006). The A_T effect is evident in the ISOW layer of the Iceland basin, which can be explained by the circulation and mixing of this layer. As ISOW flows downstream along the Reykjanes Ridge, it mixes with cLSW and NADW (van Aken and de Boer, 1995; Fogelqvist et al., 2003). The reduced volume of cLSW since mid-90s (Lazier et al., 2002; Yashayaev, 2007) has increased the importance of NADW (with high A_T; Fig. 2h) in the ISOW layer, making the pH decrease of the ISOW layer of the Iceland basin lower than in the Irminger basin.

The DIC increase (Fig. 5c,d) is the main cause of the observed pH decreases, and corresponds to pH drops between -0.00085 and -0.00134 pH units·yr^{-1} (Table 3). The waters in both the Irminger and Iceland basins gained DIC in response to the increase in atmospheric CO_2; the convection processes occurring in these basins (Pickart et al., 2003; Thierry et al., 2008; de Boisséson et al., 2010; García-Ibáñez et al., 2015; Fröb et al., 2016; Piron et al., 2016) and in the surrounding ones (i.e., Labrador and Nordic Seas) provide an important pathway for DIC to pass from the surface mixed layer to the intermediate and deep layers. The effect of the DIC increase on pH is generally dominated by the anthropogenic component (Table 3). The exception comes with the cLSW layer of the Irminger basin, where dominates the natural component resulting from the aging of the layer. All layers have higher C_{ant} increase rates in the Irminger basin than in the Iceland basin (Fig. 6a,b), and therefore larger pH declines, presumably a result of the proximity of the Irminger basin to the regions of deep water formation. The highest C_{ant} increase rates are found in the SPMW layer, owing to its direct contact with the atmosphere, and result in the highest rates of pH decrease. The higher pH drops related to C_{ant} increase found in the SPMW layer in the Irminger basin compared to those found in the Iceland basin layer, can be related to the differences in the rise in C_{ant} levels in both basins. In the Irminger basin, the rise in C_{ant} levels of the SPMW layer correspond to about 85% of the rate expected from a surface ocean maintaining its degree of saturation with the atmospheric CO_2 rise (computed using as reference the measurements of Mauna Loa), while in the Iceland basin, this rate is about 73% of the expected rate. The lower fraction in the Iceland basin compared to the Irminger basin is a consequence of the inclusion of the aforementioned poorly ventilated thermocline waters in our SPMW layer (Fig. 2e,h). Note than none of the C_{ant} trends of the SPMW layers correspond to 100% of the rate expected from assuming saturation with the atmospheric CO_2 rise. This can be explained by the fact that surface waters CO_2 concentration rise lags that of the atmosphere by between two to five years in this region (Biastoch et al., 2007; Jones et al., 2014). We also note that the temperature and A_T changes impact the pH of SPMW, decreasing and increasing it, respectively. This could indicate the increasing presence of warmer and more saline (with higher A_T) waters of subtropical origin, which, because A_T effects dominate, in last instance counteracts the effects of increasing DIC values. Overall this change can be explained as the result of the contraction of the subpolar gyre that took place since mid-90s (e.g., Flatau et al., 2003; Häkkinen and Rhines, 2004; Böning et al., 2006). Wakita et al. (2013) also found lower than expected acidification rates in the surface waters of the Pacific Ocean, which they explained as being the consequence of increasing A_T. Finally, the strong

influence of anthropogenic component on the pH decrease of the DSOW layer stands out, and is the main agent of the pH decline in this layer.

The pH change related to C_{nat} changes (Fig. 6c,d) can be interpreted as changes related to ventilation of water masses and water mass changes (with different A_T and DIC). Higher pH decreases related to C_{nat} changes indicate lack of ventilation and accumulation of DIC from remineralised organic material. This is clearly the case for the cLSW layer, where the observed pH decrease is caused by a combination of the effects of C_{ant} and C_{nat}. The greater influence of C_{nat} in the cLSW layer is the result of the aging of this water mass after its last formation event, in the mid-90s (eg., Lazier et al., 2002; Azetsu-Scott et al., 2003; Kieke et al., 2007; Yashayaev, 2007). C_{nat} also contributes to pH changes in the ISOW layer of the Iceland basin, which is related to the increasing influence of the relatively old NADW over time due to the decreasing contribution of LSW (Sy et al., 1997; Yashayaev, 2007; Sarafanov et al., 2010; García-Ibáñez et al., 2015).

4 CONCLUSIONS

The progressive acidification of the North Atlantic waters has been assessed from direct observations obtained over the last three decades (1981–2015), with the greatest pH decreases observed in surface and intermediate waters. By separating the observed pH change into its main drivers, we corroborate that the observed pH decreases are a consequence of the oceanic C_{ant} uptake and in addition we find that they have been partially offset by A_T increases. However, while the C_{ant} concentration of the upper layer roughly keeps up with that expected from rising atmospheric CO_2, the pH decreases at a lower rate than expected from C_{ant} increase. The increasing arrival of salty and alkaline subtropical waters transported by the NAC to the study region related to the contraction of the subpolar gyre since mid-90's buffers the acidification caused by the C_{ant} increase in the upper layer. The acidification rates in intermediate waters are similar to those in the surface waters, and are caused by a combination of anthropogenic and non-anthropogenic components. The acidification of cLSW due to the C_{ant} uptake is reinforced by the aging of this water mass from the end of the 1990s onwards. The pH of the deep waters of the Irminger basin, DSOW, has clearly decreased in response to anthropogenic forcing. We also observe that water mass warming contributes between 13 and 18% to the pH decrease of the upper and intermediate waters of the Irminger basin, and 34% to the pH decrease of the upper waters of the Iceland basin.

Author Contributions

All authors contributed extensively to the work presented in this paper. M.I.G.-I., A.F.R., H.M., A.O. and F.F.P. designed the research. M.I.G.-I., P.Z., F.F., L.I.C., A.F.R., H.M., A.O. and F.F.P. analysed the physical and chemical data. M.I.G.-I. and P.Z. developed the code for processing the data. M.I.G.-I. and F.F.P. determined the anthropogenic CO_2 concentrations, average layer properties and rates, and estimated the uncertainties. M.I.G.-I. wrote the manuscript and prepared all figures, with contributions from all co-authors.

Acknowledgements

We are grateful to the captains, staff and researchers who contributed to the acquisition and processing of hydrographic data. The research leading to these results was supported through the EU FP7 project

CARBOCHANGE "Changes in carbon uptake and emissions by oceans in a changing climate", which received funding from the European Commission's Seventh Framework Programme under grant agreement no. 264879. For this work M.I. Garcia-Ibáñez, A.F. Rios and F.F. Pérez were supported by the Spanish Ministry of Economy and Competitiveness (BES-2011-045614) through the CATARINA (CTM2010-17141) and BOCATS (CTM2013-41048-P) projects both co-funded by the Fondo Europeo de Desarrollo Regional 2007-2012 (FEDER). P. Zunino was supported by the GEOVIDE project as well as by IFREMER. L.I. Carracedo was funded by the University of Vigo, through the Galician I2C Plan for postdoctoral research. H. Mercier was supported by the French National Centre for Scientific Research (CNRS). F. Fröb and A. Olsen were supported by a grant from the Norwegian Research Council (SNACS, project 229756/E10).

References

Álvarez, M., Ríos, A.F., Pérez, F.F., Bryden, H.L., and Rosón, G.: Transports and budgets of total inorganic carbon in the subpolar and temperate North Atlantic, Glob. Biogeochem. Cycles, 17, 1002, doi:10.1029/2002GB001881, 2003.

Anderson, L.G. and Olsen, A.: Air–sea flux of anthropogenic carbon dioxide in the North Atlantic, Geophys. Res. Lett., 29, 1835, doi: 10.1029/2002GL014820, 2002.

Azetsu-Scott, K., Jones, E.P., Yashayaev, I., and Gershey, R.M.: Time series study of CFC concentrations in the Labrador Sea during deep and shallow convection regimes (1991–2000), J. Geophys. Res., 108, 3354, doi:10.1029/2002JC001317, 2003.

Bates, N., Astor, Y., Church, M., Currie, K., Dore, J., Gonaález-Dávila, M., Lorenzoni, L., Muller-Karger, F., Olafsson, J., and Santa-Casiano, M.: A Time-Series View of Changing Ocean Chemistry Due to Ocean Uptake of Anthropogenic CO_2 and Ocean Acidification, Oceanography, 27, 126–141, doi:10.5670/oceanog.2014.16, 2014.

Bates, N.R., Best, M.H.P., Neely, K., Garley, R., Dickson, A.G., and Johnson, R.J.: Detecting anthropogenic carbon dioxide uptake and ocean acidification in the North Atlantic Ocean, Biogeosciences, 9, 2509–2522, doi:10.5194/bg-9-2509-2012, 2012.

Benson, B.B. and Krause, D.: The concentration and isotopic fractionation of oxygen dissolved in freshwater and seawater in equilibrium with the atmosphere, Limnol. Oceanogr., 29, 620–632, doi:10.4319/lo.1984.29.3.0620, 1984.

Bersch, M., Meincke, J., and Sy, A.: Interannual thermohaline changes in the northern North Atlantic 1991–1996, Deep Sea Res. Part II Top. Stud. Oceanogr., 46, 55–75, doi:10.1016/S0967-0645(98)00114-3, 1999.

Biastoch, A., Völker, C., and Böning, C.W.: Uptake and spreading of anthropogenic trace gases in an eddy-permitting model of the Atlantic Ocean, J. Geophys. Res., 112, C09017, doi:10.1029/2006JC003966, 2007.

Böning, C.W., Scheinert, M., Dengg, J., Biastoch, A., and Funk, A.: Decadal variability of subpolar gyre transport and its reverberation in the North Atlantic overturning, Geophys. Res. Lett., 33, L21S01, doi:10.1029/2006GL026906, 2006.

Bradshaw, A., Brewer, P., Shafer, D., and Williams, R.: Measurements of total carbon dioxide and alkalinity by potentiometric titration in the GEOSECS program, Earth Planet. Sci. Lett., 55, 99–115, doi:10.1016/0012-821X(81)90090-X, 1981.

Brambilla, E. and Talley, L.D.: Subpolar Mode Water in the northeastern Atlantic: 1. Averaged properties and mean circulation, J. Geophys. Res., 113, C04025, doi:10.1029/2006JC004062, 2008.

Brewer, P.G., Takahashi, T., and Williams, R.T.: Transient tracers in the ocean (TTO) - Hydrographic data and carbon dioxide systems with revised carbon chemistry data, NDP-004/R, Carbon Dioxide Information Center, Oak Ridge National Laboratory, Oak Ridge, TN, 28 pp., doi:10.2172/538035, 1986.

Caldeira, K. and Wickett, M.E.: Oceanography: Anthropogenic carbon and ocean pH, Nature, 425, 365–365, doi:10.1038/425365a, 2003.

Caldeira, K. and Wickett, M.E.: Ocean model predictions of chemistry changes from carbon dioxide emissions to the atmosphere and ocean, J. Geophys. Res., 110, C09S04, doi:10.1029/2004JC002671, 2005.

Carter, B.R., Radich, J.A., Doyle, H.L., and Dickson, A.G.: An automated system for spectrophotometric seawater pH measurements, Limnol. Oceanogr. Methods, 11, 16–27, doi:10.4319/lom.2013.11.16, 2013.

Ciais, P., Sabine, C., Bala, G., Bopp, L., Brovkin, V., Canadell, J., Chhabra, A., DeFries, R., Galloway, J., Heimann, M., Jones, C., Le Quéré, C., Myneni, R.B., Piao, S., and Thornton, P.: Carbon and other biogeochemical cycles, in: Climate Change 2013: The Physical Science Basis. Contribution of Working Group I to the Fifth Assessment Report of the Intergovernmental Panel on Climate Change [Stocker, T.F., Qin, D., Plattner, G.-K., Tignor, M., Allen, S.K., Boschung, J., Nauels, A., Xia, Y., Bex V., and Midgley, P.M. (eds.)], Cambridge University Press, Cambridge, United Kingdom and New York, NY, USA. 465–570, 2013.

Clayton, T.D. and Byrne, R.H.: Spectrophotometric seawater pH measurements: total hydrogen ion concentration scale calibration of m-cresol purple and at-sea results, Deep Sea Res. Part I: Oceanogr. Res. Pap., 40, 2115–2129, doi:10.1016/0967-0637(93)90048-8, 1993.

de Boisséson, E., Thierry, V., Mercier, H., and Caniaux, G.: Mixed layer heat budget in the Iceland Basin from Argo, J. Geophys. Res. Oceans, 115, C10055, doi:10.1029/2010JC006283, 2010.

Desbruyères, D., Thierry, V., and Mercier, H.: Simulated decadal variability of the meridional overturning circulation across the A25-Ovide section, J. Geophys. Res. Oceans, 118, 462–475, doi:10.1029/2012JC008342, 2013.

DeVries, T.: The oceanic anthropogenic CO_2 sink: Storage, air-sea fluxes, and transports over the industrial era, Glob. Biogeochem. Cycles, 28, 631–647, doi:10.1002/2013GB004739, 2014.

Dickson, A.G.: The measurement of sea water pH, Mar. Chem., 44, 131–142, doi:10.1016/0304-4203(93)90198-W, 1993a

Dickson, A.G.: pH buffers for sea water media based on the total hydrogen ion concentration scale, Deep Sea Res. Part I: Oceanogr. Res. Pap., 40, 107–118, doi:10.1016/0967-0637(93)90055-8, 1993b.

Dickson, A. and Goyet, C.: Handbook of methods for the analysis of the various parameters of the carbon dioxide system in sea water. Version 2, Oak Ridge National Laboratory, Oak Ridge, TN, 198 pp., doi:10.2172/10107773, 1994.

Dickson, A.G., Sabine, C.L., and Christian, J.R.: Guide to best practices for ocean CO_2 measurements, PICES Spec. Publ., 3, North Pacific Marine Science Organization Sidney, British Columbia, 191 pp., 2007.

Dickson, A. and Millero, F.: A comparison of the equilibrium constants for the dissociation of carbonic acid in seawater media, Deep-Sea Res., 34, 1733–1743, doi:10.1016/0198-0149(87)90021-5, 1987.

Doney, S.C., Fabry, V.J., Feely, R.A., and Kleypas, J.A.: Ocean acidification: the other CO_2 problem, Annu. Rev. Mar. Sci., 1, 169–192, doi:10.1146/annurev.marine.010908.163834, 2009.

Dore, J.E., Lukas, R., Sadler, D.W., Church, M.J., and Karl, D.M.: Physical and biogeochemical modulation of ocean acidification in the central North Pacific, Proc. Natl. Acad. Sci., 106, 12235–12240, doi:10.1073/pnas.0906044106, 2009.

Eakins, B.W. and Sharman, G.F.: Volumes of the World's Oceans from ETOPO1, NOAA National Geophysical Data Center, Boulder, CO, 2010.

Feely, R.A., Doney, S.C., and Cooley, S.R.: Ocean acidification: Present and future changes in a high-CO_2 world, Oceanography, 22, 36–47, doi:10.5670/oceanog.2009.95, 2009.

Feely, R.A., Sabine, C.L., Lee, K., Berelson, W., Kleypas, J., Fabry, V.J., and Millero, F.J.: Impact of Anthropogenic CO_2 on the $CaCO_3$ System in the Oceans, Science, 305, 362–366, doi:10.1126/science.1097329, 2004.

Flatau, M.K., Talley, L., and Niiler, P.P.: The North Atlantic Oscillation, Surface Current Velocities, and SST Changes in the Subpolar North Atlantic, J. Clim., 16, 2355–2369, doi:10.1175/2787.1, 2003.

Fogelqvist, E., Blindheim, J., Tanhua, T., Østerhus, S., Buch, E., and Rey, F.: Greenland–Scotland overflow studied by hydro-chemical multivariate analysis, Deep Sea Res. Part I: Oceanogr. Res. Pap., 50, 73–102, doi:10.1016/S0967-0637(02)00131-0, 2003.

Fröb, F., Olsen, A., Våge, K., Moore, K., Yashayaev, I., Jeannson, E., and Rajasakaren, B.: Record deep convection in the Irminger Sea in winter 2014-15, OSM, New Orleans, Louisiana, USA, 21-16 February 2016, HE11A-02, 2016.

García-Ibáñez, M.I., Pardo, P.C., Carracedo, L.I., Mercier, H., Lherminier, P., Ríos, A.F., and Pérez, F.F.: Structure, transports and transformations of the water masses in the Atlantic Subpolar Gyre, Prog. Oceanogr., 135, 18–36, doi:10.1016/j.pocean.2015.03.009, 2015.

Gattuso, J.-P., Brewer, P.G., Hoegh-Guldberg, O., Kleypas, J.A., Pörtner, H.-O., and Schmidt, D.N.: Cross-chapter box on ocean acidification, in: IPCC, 2014: Climate Change 2014: Impacts, Adaptation, and Vulnerability. Part A: Global and Sectoral Aspects. Contribution of Working Group II to the Fifth Assessment Report of the Intergovernmental Panel on Climate Change [Field, C.B., Barros, V.R., Dokken, D.J., Mach, K.J., Mastrandrea, M.D., Bilir, T.E., Chatterjee, M., Ebi, K.L., Estrada, Y.O., Genova, R.C., Girma, B., Kissel, E.S., Levy, A.N., MacCracken, S., Mastrandrea, P.R., and White, L.L. (eds.)], Cambridge University Press, Cambridge, United Kingdom and New York, NY, USA, 129–13, 2014.

Gehlen, M., Gruber, N., Gangstø, R., Bopp, L., and Oschlies, A.: Biogeochemical consequences of ocean acidification and feedbacks to the earth system, in: Ocean Acidification, Vol. 1 [Gattuso, J.-P. and Hansson, L. (eds.)], Oxford University Press, 230–248, 2011.

González-Dávila, M., Santana-Casiano, J.M., Rueda, M.J., and Llinás, O.: The water column distribution of carbonate system variables at the ESTOC site from 1995 to 2004, Biogeosciences, 7, 3067–3081, doi:10.5194/bg-7-3067-2010, 2010.

Gourcuff, C., Lherminier, P., Mercier, H., and Le Traon, P.Y.: Altimetry Combined with Hydrography for Ocean Transport Estimation, J. Atmospheric Ocean. Technol., 28, 1324–1337, doi:10.1175/2011JTECHO818.1, 2011.

Guallart, E.F., Fajar, N.M., Padín, X.A., Vázquez-Rodríguez, M., Calvo, E., Ríos, A.F., Hernández-Guerra, A., Pelejero, C., and Pérez, F.F.: Ocean acidification along the 24.5°N section in the subtropical North Atlantic, Geophys. Res. Lett., 42, 2014GL062971, doi:10.1002/2014GL062971, 2015.

Häkkinen, S. and Rhines, P.B.: Decline of subpolar North Atlantic circulation during the 1990s, Science, 304, 555–559, doi:10.1126/science.1094917, 2004.

Johnson, K.M., Wills, K.D., Butler, D.B., Johnson, W.K., and Wong, C.S.: Coulometric total carbon dioxide analysis for marine studies: maximizing the performance of an automated gas extraction system and coulometric detector, Mar. Chem., 44, 167–187, doi:10.1016/0304-4203(93)90201-X, 1993.

Jones, D.C., Ito, T., Takano, Y., and Hsu, W.-C.: Spatial and seasonal variability of the air-sea equilibration timescale of carbon dioxide, Glob. Biogeochem. Cycles, 28, 1163–1178, doi:10.1002/2014GB004813, 2014.

Khatiwala, S., Tanhua, T., Mikaloff Fletcher, S., Gerber, M., Doney, S.C., Graven, H.D., Gruber, N., McKinley, G.A., Murata, A., Ríos, A.F., and Sabine, C.L.: Global ocean storage of anthropogenic carbon, Biogeosciences, 10, 2169–2191, doi:10.5194/bg-10-2169-2013, 2013.

Kieke, D., Rhein, M., Stramma, L., Smethie, W.M., Bullister, J.L., and LeBel, D.A.: Changes in the pool of Labrador Sea Water in the subpolar North Atlantic, Geophys. Res. Lett., 34, L06605, doi:10.1029/2006GL028959, 2007.

Koltermann, K.P., Pfannkuche, O., and Meincke, J.: JGOFS, OMEX and WOCE in the North Atlantic 1994, cruise no. 30: 7 September-22 December 1994, Meteor-Berichte, 96-3, Universität Hamburg, 148 pp., 1996.

Langdon, C., Takahashi, T., Sweeney, C., Chipman, D., Goddard, J., Marubini, F., Aceves, H., Barnett, H., and Atkinson, M.J.: Effect of calcium carbonate saturation state on the calcification rate of an experimental coral reef, Glob. Biogeochem. Cycles, 14, 639–654, doi:10.1029/1999GB001195, 2000.

Lazier, J., Hendry, R., Clarke, A., Yashayaev, I., and Rhines, P.: Convection and restratification in the Labrador Sea, 1990–2000, Deep Sea Res. Part I: Oceanogr. Res. Pap., 49, 1819–1835, doi:10.1016/S0967-0637(02)00064-X, 2002.

Le Quéré, C., Moriarty, R., Andrew, R.M., Canadell, J.G., Sitch, S., Korsbakken, J.I., Friedlingstein, P., Peters, G.P., Andres, R.J., Boden, T.A., Houghton, R.A., House, J.I., Keeling, R.F., Tans, P., Arneth, A., Bakker, D.C.E., Barbero, L., Bopp, L., Chang, J., Chevallier, F., Chini, L.P., Ciais, P., Fader, M., Feely, R.A., Gkritzalis, T., Harris, I., Hauck, J., Ilyina, T., Jain, A.K., Kato, E., Kitidis, V., Klein Goldewijk, K., Koven, C., Landschützer, P., Lauvset, S.K., Lefèvre, N., Lenton, A., Lima, I.D., Metzl, N., Millero, F., Munro, D.R., Murata, A., Nabel, J.E.M.S., Nakaoka, S., Nojiri, Y., O'Brien, K., Olsen, A., Ono, T., Pérez, F.F., Pfeil, B., Pierrot, D., Poulter, B., Rehder, G., Rödenbeck, C., Saito, S., Schuster, U., Schwinger, J., Séférian, R., Steinhoff, T., Stocker, B.D., Sutton, A.J., Takahashi, T., Tilbrook, B., van der Laan-Luijkx, I.T., van der Werf, G.R., van Heuven, S., Vandemark, D., Viovy, N., Wiltshire, A., Zaehle, S., and Zeng, N.: Global Carbon Budget 2015, Earth Syst. Sci. Data, 7, 349–396, doi:10.5194/essd-7-349-2015, 2015.

Lherminier, P., Mercier, H., Gourcuff, C., Alvarez, M., Bacon, S., and Kermabon, C.: Transports across the 2002 Greenland-Portugal Ovide section and comparison with 1997, J. Geophys. Res., 112, C07003, doi:10.1029/2006JC003716, 2007.

Lherminier, P., Mercier, H., Huck, T., Gourcuff, C., Perez, F.F., Morin, P., Sarafanov, A., and Falina, A.: The Atlantic Meridional Overturning Circulation and the subpolar gyre observed at the A25-OVIDE section in June 2002 and 2004, Deep Sea Res. Part I: Oceanogr. Res. Pap., 57, 1374–1391, doi:10.1016/j.dsr.2010.07.009, 2010.

Liu, X., Patsavas, M.C., and Byrne, R.H.: Purification and Characterization of meta-Cresol Purple for Spectrophotometric Seawater pH Measurements, Environ. Sci. Technol., 45, 4862–4868, doi:10.1021/es200665d, 2011.

Maier-Reimer, E. and Hasselmann, K.: Transport and storage of CO_2 in the ocean—an inorganic ocean-circulation carbon cycle model, Clim. Dyn., 2, 63–90, doi:10.1007/BF01054491, 1987.

Matear, R.J. and Lenton, A.: Quantifying the impact of ocean acidification on our future climate, Biogeosciences, 11, 3965–3983, doi:10.5194/bg-11-3965-2014, 2014.

Mehrbach, C., Culberson, C.H., Hawley, J.E., and Pytkowicz, R.M.: Measurement of the apparent dissociation constants of carbonic acid in seawater at atmospheric pressure, Limnol. Oceanogr., 18, 897–907, doi:10.4319/lo.1973.18.6.0897, 1973.

Meincke, J. and Becker, G.: WOCE-NORD, Cruise No. 18, 2 September-26 September 1991. Nordsee, cruise No. 19, 30 September-12 October 1991. METEOR-Berichte 93-1, Univ. Hambg., 105 pp., 1993.

Mercier, H., Lherminier, P., Sarafanov, A., Gaillard, F., Daniault, N., Desbruyères, D., Falina, A., Ferron, B., Gourcuff, C., and Huck, T.: Variability of the meridional overturning circulation at the Greenland–Portugal OVIDE section from 1993 to 2010, Prog. Oceanogr., 132, 250–261, doi:10.1016/j.pocean.2013.11.001, 2015.

Millero, F.J., Zhang, J.Z., Lee, K., and Campbell, D.M.: Titration alkalinity of seawater, Mar. Chem., 44, 153–165, doi:10.1016/0304-4203(93)90200-8, 1993.

Mintrop, L., Pérez, F.F., González-Dávila, M., Santana-Casiano, J.M., and Körtzinger, A.: Alkalinity determination by potentiometry: Intercalibration using three different methods, Cienc. Mar., 26, 23–37, doi:10.7773/cm.v26i1.573, 2000.

Olafsson, J., Olafsdottir, S.R., Benoit-Cattin, A., Danielsen, M., Arnarson, T.S., and Takahashi, T.: Rate of Iceland Sea acidification from time series measurements, Biogeosciences, 6, 2661–2668, doi:10.5194/bg-6-2661-2009, 2009.

Olafsson, J., Olafsdottir, S.R., Benoit-Cattin, A., Takahashi, T.: The Irminger Sea and the Iceland Sea time series measurements of sea water carbon and nutrient chemistry 1983–2008, Earth Syst. Sci. Data, 2, 99–104, doi:10.5194/essd-2-99-2010, 2010.

Olsen, A., Abdirahman, O.M., Bellerby, R.G., Johannessen, T., Ninnemann, U.S., Brown, K.R., Olsson, K.A., Olafsson, J., Nondal, G., Kivimäe, C., Kringstad, S., Neill, C., Olafsdottir, S.: Magnitude and Origin of the Anthropogenic CO_2 Increase and the ^{13}C Suess Effect in the Nordic Seas since 1981, Glob. Biogeochem. Cycles, 20, GB3027, doi:10.1029/2005GB002669, 2006.

Olsen, A., Key, R.M., Heuven, S. van, Lauvset, S.K., Velo, A., Lin, X., Schirnick, C., Kozyr, A., Tanhua, T., Hoppema, M., Jutterström, S., Steinfeldt, R., Jeansson, E., Ishii, M., Pérez, F.F., and Suzuki, T.: An internally consistent data product for the world ocean: the Global Ocean Data Analysis Project, version 2 (GLODAPv2), Earth Syst. Sci. Data Discuss., doi:10.5194/essd-2015-42 , in review, 2016.

Ono, T., Watanabe, S., Okuda, K., and Fukasawa, M.: Distribution of total carbonate and related properties in the North Pacific along 30°N, J. Geophys. Res. Oceans, 103, 30873–30883, doi:10.1029/1998JC900018, 1998.

Orr, J.C.: Recent and future changes in ocean carbonate chemistry, in: Ocean Acidification, Vol. 1, [Gattuso, J.-P. and Hansson, L. (eds.)], Oxford University Press, 41–66, 2011.

Orr, J.C., Fabry, V.J., Aumont, O., Bopp, L., Doney, S.C., Feely, R.A., Gnanadesikan, A., Gruber, N., Ishida, A., Joos, F., Key, R.M., Lindsay, K., Maier-Reimer, E., Matear, R., Monfray, P., Mouchet, A., Najjar, R.G., Plattner, G.-K., Rodgers, K.B., Sabine, C.L., Sarmiento, J.L., Schlitzer, R., Slater, R.D., Totterdell, I.J., Weirig, M.F., Yamanaka, Y., and Yool, A.: Anthropogenic ocean acidification over the twenty-first century and its impact on calcifying organisms, Nature, 437, 681–686, doi:10.1038/nature04095, 2005.

Pérez, F.F. and Fraga, F.: A precise and rapid analytical procedure for alkalinity determination, Mar. Chem., 21, 169–182, doi:10.1016/0304-4203(87)90037-5, 1987.

Pérez, F.F., Mercier, H., Vázquez-Rodríguez, M., Lherminier, P., Velo, A., Pardo, P.C., Rosón, G., and Ríos, A.F.: Atlantic Ocean CO_2 uptake reduced by weakening of the meridional overturning circulation, Nat. Geosci., 6, 146–152, doi:10.1038/ngeo1680, 2013.

Pérez, F.F., Vázquez-Rodríguez, M., Louarn, E., Padín, X.A., Mercier, H., and Ríos, A.F.: Temporal variability of the anthropogenic CO_2 storage in the Irminger Sea, Biogeosciences, 5, 1669–1679, doi:10.5194/bg-5-1669-2008, 2008.

Pérez, F.F., Vázquez-Rodríguez, M., Mercier, H., Velo, A., Lherminier, P., and Ríos, A.F.: Trends of anthropogenic CO_2 storage in North Atlantic water masses, Biogeosciences, 7, 1789–1807, doi:10.5194/bg-7-1789-2010, 2010.

Pickart, R.S., Straneo, F., and Moore, G.K.: Is Labrador Sea Water formed in the Irminger basin?, Deep Sea Res. Part I: Oceanogr. Res. Pap., 50, 23–52, doi:10.1016/S0967-0637(02)00134-6, 2003.

Piron, A., Thierry, V., Mercier, H., and Caniaux, G.: Argo float observations of basin-scale deep convection in the Irminger sea during winter 2011-2012, Deep Sea Res. Part I: Oceanogr. Res. Pap., 109, 76–90, doi:10.1016/j.dsr.2015.12.012, 2016.

Pörtner, H.O., Langenbuch, M., and Reipschläger, A.: Biological Impact of Elevated Ocean CO_2 Concentrations: Lessons from Animal Physiology and Earth History, J. Oceanogr., 60, 705–718, doi:10.1007/s10872-004-5763-0, 2004.

Quay, P., Sonnerup, R., Stutsman, J., Maurer, J., Körtzinger, A., Padin, X.A., and Robinson, C.: Anthropogenic CO_2 accumulation rates in the North Atlantic Ocean from changes in the $^{13}C/^{12}C$ of dissolved inorganic carbon, Glob. Biogeochem. Cycles, 21, GB1009, doi:10.1029/2006GB002761, 2007.

Raven, J., Caldeira, K., Elderfield, H., Hoegh-Guldberg, O., Liss, P., Riebesell, U., Shepherd, J., Turley, C., and Watson, A.: Ocean acidification due to increasing atmospheric carbon dioxide, R. Soc. Lond. Document No. 12/05, The Royal Society, London, 2005.

Rhein, M., Fischer, J., Smethie, W.M., Smythe-Wright, D., Weiss, R.F., Mertens, C., Min, D.-H., Fleischmann, U., and Putzka, A.: Labrador Sea Water: Pathways, CFC inventory, and formation rates, J. Phys. Oceanogr., 32, 648–665, doi:10.1175/1520-0485(2002)032<0648:LSWPCI>2.0.CO;2, 2002.

Riebesell, U., Zondervan, I., Rost, B., Tortell, P.D., Zeebe, R.E., and Morel, F.M.M.: Reduced calcification of marine plankton in response to increased atmospheric CO_2, Nature, 407, 364–367, doi:10.1038/35030078, 2000.

Ríos, A.F., Álvarez-Salgado, X.A., Pérez, F.F., Bingler, L.S., Arístegui, J., and Mémery, L.: Carbon dioxide along WOCE line A14: Water masses characterization and anthropogenic entry, J. Geophys. Res. Oceans, 108, 3123, doi:10.1029/2000JC000366, 2003.

Ríos, A.F., Resplandy, L., García-Ibáñez, M.I., Fajar, N.M., Velo, A., Padin, X.A., Wanninkhof, R., Steinfeldt, R., Rosón, G., and Pérez, F.F.: Decadal acidification in the water masses of the Atlantic Ocean, Proc. Natl. Acad. Sci., 112, 9950–9955, doi:10.1073/pnas.1504613112, 2015.

Sabine, C.L., Feely, R.A., Gruber, N., Key, R.M., Lee, K., Bullister, J.L., Wanninkhof, R., Wong, C.S., Wallace, D.W.R., Tilbrook, B., Millero, F.J., Peng, T.-H., Kozyr, A., Ono, T., and Rios, A.F.: The Oceanic Sink for Anthropogenic CO_2, Science, 305, 367–371, doi:10.1126/science.1097403, 2004.

Santana-Casiano, J.M., González-Dávila, M., Rueda, M.-J., Llinás, O., and González-Dávila, E.-F.: The interannual variability of oceanic CO_2 parameters in the northeast Atlantic subtropical gyre at the ESTOC site, Glob. Biogeochem. Cycles, 21, GB1015, doi:10.1029/2006GB002788., 2007.

Sarafanov, A., Falina, A., Mercier, H., Sokov, A., Lherminier, P., Gourcuff, C., Gladyshev, S., Gaillard, F., and Daniault, N.: Mean full-depth summer circulation and transports at the northern periphery of the Atlantic Ocean in the 2000s, J. Geophys. Res., 117, C01014, doi:10.1029/2011JC007572, 2012.

Sarafanov, A., Falina, A., Sokov, A., and Demidov, A.: Intense warming and salinification of intermediate waters of southern origin in the eastern subpolar North Atlantic in the 1990s to mid-2000s, J. Geophys. Res. Oceans, 113, C12022, doi:10.1029/2008JC004975, 2008.

Sarafanov, A., Mercier, H., Falina, A., Sokov, A., and Lherminier, P.: Cessation and partial reversal of deep water freshening in the northern North Atlantic: observation-based estimates and attribution, Tellus A, 62, 80–90, doi:10.1111/j.1600-0870.2009.00418.x, 2010.

Sarmiento, J.L., Orr, J.C., and Siegenthaler, U.: A perturbation simulation of CO_2 uptake in an ocean general circulation model, J. Geophys. Res. Oceans, 97, 3621–3645, doi:10.1029/91JC02849, 1992.

Steinfeldt, R., Rhein, M., Bullister, J.L., and Tanhua, T.: Inventory changes in anthropogenic carbon from 1997–2003 in the Atlantic Ocean between 20°S and 65°N, Glob. Biogeochem. Cycles, 23, GB3010, doi:10.1029/2008GB003311, 2009.

Stoll, M.H.C., van Aken, H.M., de Baar, H.J.W., and Kraak, M.: Carbon dioxide characteristics of water masses in the northern North Atlantic Ocean, Mar. Chem., 55, 217–232, doi:10.1016/S0304-4203(96)00058-8, 1996.

Sy, A., Rhein, M., Lazier, J.R.N., Koltermann, K.P., Meincke, J., Putzka, A., and Bersch, M.: Surprisingly rapid spreading of newly formed intermediate waters across the North Atlantic Ocean, Nature, 386, 675–679, doi:10.1038/386675a0, 1997.

Takahashi, T. and Brewer, P.: Hydrographic and chemistry data for the TTO/NAS expedition, April-October, 1981: Revised carbon chemistry data Rep. NDP004, Carbon Dioxide Inf. Anal. Cent., Oak Ridge, TN, 1986.

Tanhua, T. and Wallace, D.W.R.: Consistency of TTO-NAS inorganic carbon data with modern measurements, Geophys. Res. Lett., 32, L14618, doi:10.1029/2005GL023248, 2005.

Thierry, V., de Boisséson, E., and Mercier, H.: Interannual variability of the Subpolar Mode Water properties over the Reykjanes Ridge during 1990–2006, J. Geophys. Res. Oceans, 113, C04016, doi:10.1029/2007JC004443, 2008.

van Aken, H.M. and de Boer, C.J.: On the synoptic hydrography of intermediate and deep water masses in the Iceland Basin, Deep Sea Res. Part I: Oceanogr. Res. Pap., 42, 165–189, doi:10.1016/0967-0637(94)00042-Q, 1995.

Vázquez-Rodríguez, M., Padin, X.A., Ríos, A.F., Bellerby, R.G.J., and Pérez, F.F.: An upgraded carbon-based method to estimate the anthropogenic fraction of dissolved CO_2 in the Atlantic Ocean, Biogeosciences Discuss., 6, 4527–4571, doi:10.5194/bgd-6-4527-2009, 2009a.

Vázquez-Rodríguez, M., Touratier, F., Lo Monaco, C., Waugh, D.W., Padin, X.A., Bellerby, R.G.J., Goyet, C., Metzl, N., Ríos, A.F., and Pérez, F.F.: Anthropogenic carbon distributions in the Atlantic Ocean: data-based estimates from the Arctic to the Antarctic, Biogeosciences, 6, 439–451, doi:10.5194/bg-6-439-2009, 2009b.

Vázquez-Rodríguez, M., Padin, X.A., Pardo, P.C., Ríos, A.F., and Pérez, F.F.: The subsurface layer reference to calculate preformed alkalinity and air–sea CO_2 disequilibrium in the Atlantic Ocean, J. Mar. Syst., 94, 52–63, doi:10.1016/j.jmarsys.2011.10.008, 2012a.

Vázquez-Rodríguez, M., Pérez, F.F., Velo, A., Ríos, A.F., and Mercier, H.: Observed acidification trends in North Atlantic water masses, Biogeosciences, 9, 5217–5230, doi:10.5194/bg-9-5217-2012, 2012b.

Velo, A., Pérez, F.F., Tanhua, T., Gilcoto, M., Ríos, A.F., and Key, R.M.: Total alkalinity estimation using MLR and neural network techniques, J. Mar. Syst., 111–112, 11–18, doi:10.1016/j.jmarsys.2012.09.002, 2013.

Wakita, M., Watanabe, S., Honda, M., Nagano, A., Kimoto, K., Matsumoto, K., Kitamura, M., Sasaki, K., Kawakami, H., Fujiki, T., Sasaoka, K., Nakano, Y., and Murata, A.: Ocean acidification from 1997 to 2011 in the subarctic western North Pacific Ocean, Biogeosciences, 10, 7817–7827, doi:10.5194/bg-10-7817-2013, 2013.

Wallace, W.R.: Storage and transport of excess CO_2 in the oceans: The JGOFS/WOCE global CO_2 survey, in: Ocean Circulation and Climate [Siedler, G., Church, J., and Gould J. (eds.)], Academic Press, 489–521, 2001.

Yashayaev, I.: Hydrographic changes in the Labrador Sea, 1960-2005, Prog. Oceanogr., 73, 242–276, doi:10.1016/j.pocean.2007.04.015, 2007.

Yashayaev, I., Bersch, M., and van Aken, H.M.: Spreading of the Labrador Sea Water to the Irminger and Iceland basins, Geophys. Res. Lett., 34, L10602, doi:10.1029/2006GL028999, 2007.

Yashayaev, I., Holliday, N.P., Bersch, M., and van Aken, H.M.: The History of the Labrador Sea Water: Production, Spreading, Transformation and Loss, in: Arctic–Subarctic Ocean Fluxes: Defining the Role of the Northern Seas in Climate [Dickson, R.R., Meincke, J., and Rhines, P. (eds.)], Springer Netherlands, 569–612, 2008.

Zunino, P., Pérez, F.F., Fajar, N.M., Guallart, E.F., Ríos, A.F., Pelegrí, J.L., and Hernández-Guerra, A.: Transports and budgets of anthropogenic CO_2 in the tropical North Atlantic in 1992–1993 and 2010–2011, Glob. Biogeochem. Cycles, 29, 2014GB005075, doi:10.1002/2014GB005075, 2015.

Biogeosciences Discuss., doi:10.5194/bg-2016-66, 2016
Manuscript under review for journal Biogeosciences
Published: 29 February 2016

Table 1: List of hydrographic cruises used in this study (Fig. 1a). P.I. denotes principal investigator, and #St the number of stations selected.

Cruise Name	Expocode	Month/Year	Vessel	P.I.	#St	Reference
TTO-NAS L6	316N19810821	08–09/1981	*Knorr*	W.J. Jenkins	11	Takahashi and Brewer (1986)
AR07E	64TR91_1	04–05/1991	*Tyro*	H.M. van Aken	12	Stoll et al. (1996)
A01E	06MT18_1	09/1991	*Meteor*	J. Meincke	15	Meincke and Becker (1993)
A01E	06MT30_3	11–12/1994	*Meteor*	J. Meincke	27	Koltermann et al. (1996)
AR07E	06MT39_5	08–09/1997	*Meteor*	A. Sy	32	Rhein et al. (2002)
OVIDE 2002	35TH20020610	06–07/2002	*Thalassa*	H. Mercier	38	Lherminier et al. (2007)
OVIDE 2004	35TH20040604	06–07/2004	*Thalassa*	T. Huck	56	Lherminier et al. (2010)
OVIDE 2006	06MM20060523	05–06/2006	*Maria S. Merian*	P. Lherminier	44	Gourcuff et al. (2011)
OVIDE 2008	35TH20080610	06–07/2008	*Thalassa*	H. Mercier	45	Mercier et al. (2015)
OVIDE 2010	35TH20100610	06/2010	*Thalassa*	T. Huck; H. Mercier	46	Mercier et al. (2015)
CATARINA[a]	29AH20120623	06–07/2012	*Sarmiento de Gamboa*	A.F. Ríos	44	This work
GEOVIDE[a]	35PQ20140517	05–06/2014	*Pourquoi Pas?*	G. Sarthou	31	This work
58GS20150410	58GS20150410	04-05/2015	*G.O. Sars*	A. Olsen	10	Fröb et al. (2016)

[a]Both CATARINA (http://catarina.iim.csic.es/en) and GEOVIDE (http://www.geovide.obs-vlfr.fr) cruises contain the OVIDE section (http://wwz.ifremer.fr/lpo/La-recherche/Projets-en-cours/OVIDE), and in the study are referred as OVIDE 2012 and 2014, respectively.

Biogeosciences Discuss., doi:10.5194/bg-2016-66, 2016
Manuscript under review for journal Biogeosciences
Published: 29 February 2016

Table 2: Mean values ± confidence interval of pressure (in dbar), potential temperature (θ, in ºC), salinity, Apparent Oxygen Utilization (AOU, in µmol·kg^{-1}), total alkalinity (A_T, in µmol·kg^{-1}), anthropogenic CO_2 (C_{ant}, in µmol·kg^{-1}) and pH at total scale and 25ºC (pH_{T25}) for the bottom waters of the Iberian Abyssal Plain sampled during the seven OVIDE cruises. "n" represents the number of data considered in each cruise. The last row represents the inter-cruise confidence interval (i.e., the confidence interval of the mean values across the seven cruises).

Year (n)	Pressure	θ	Salinity	AOU	A_T	C_{ant}	pH_{T25}
2002 (144)	4205 ± 1052	2.182 ± 0.160	34.913 ± 0.016	86.1 ± 4.0	2351 ± 6	6.4 ± 2.6	7.740 ± 0.006
2004 (158)	4263 ± 998	2.162 ± 0.150	34.908 ± 0.014	87.1 ± 2.8	2352 ± 6	6.2 ± 2.4	7.741 ± 0.006
2006 (132)	4252 ± 1058	2.170 ± 0.164	34.913 ± 0.016	85.4 ± 3.2	2350 ± 6	6.2 ± 2.6	7.741 ± 0.006
2008 (125)	4206 ± 1022	2.179 ± 0.150	34.911 ± 0.014	84.9 ± 3.6	2353 ± 8	7.0 ± 3.2	7.744 ± 0.006
2010 (131)	4312 ± 1048	2.163 ± 0.154	34.908 ± 0.016	85.9 ± 3.2	2351 ± 6	7.0 ± 2.4	7.740 ± 0.004
2012 (102)	4397 ± 1052	2.149 ± 0.154	34.909 ± 0.016	87.9 ± 3.2	2352 ± 6	5.1 ± 2.4	7.742 ± 0.004
2014 (54)	4441 ± 954	2.141 ± 0.138	34.904 ± 0.014	87.4 ± 2.6	2353 ± 6	5.5 ± 3.0	7.743 ± 0.006
	70	0.011	0.002	0.8	0.8	0.5	0.001

Biogeosciences Discuss., doi:10.5194/bg-2016-66, 2016
Manuscript under review for journal Biogeosciences
Published: 29 February 2016

Table 3: Observed temporal changes of pH at total scale and in situ conditions (in situ temperature and pressure; $\frac{dpH_{Tis}}{dt}$ obs) for the main water masses in the Irminger and Iceland basins for the period 1981–2015. pH changes caused by the main drivers (in situ temperature, T_{is}; salinity, S; total alkalinity, A_T; total dissolved inorganic carbon, DIC; anthropogenic CO_2, C_{ant}; natural DIC, C_{nat}) are also shown, as well as the pH changes result of the sum of the pH changes caused by the individual drivers ($\frac{dpH_{Tis}}{dt}$ model). All the trends are calculated based on the annually interpolated values and are in 10^{-3} pH units·yr^{-1}. Values in parenthesis are the percentages of the observed pH change explained by each one of its drivers. Confront Fig. 1 for water mass acronyms.

		$\frac{dpH_{Tis}}{dt}$ obs	$\frac{\partial pH_{Tis}}{\partial T_{is}}\frac{dT_{is}}{dt}$	$\frac{\partial pH_{Tis}}{\partial S}\frac{dS}{dt}$	$\frac{\partial pH_{Tis}}{\partial A_T}\frac{dA_T}{dt}$	$\frac{\partial pH_{Tis}}{\partial DIC}\frac{dDIC}{dt}$	$\frac{\partial pH_{Tis}}{\partial DIC}\frac{dC_{ant}}{dt}$	$\frac{\partial pH_{Tis}}{\partial DIC}\frac{dC_{nat}}{dt}$	$\frac{dpH_{Tis}}{dt}$ model
Irminger	SPMW	-1.31 ± 0.08	-0.24 ± 0.06 (18)	-0.02 ± 0.01 (2)	0.29 ± 0.05 (-22)	-1.34 ± 0.12 (102)	-1.59 ± 0.10 (121)	0.24 ± 0.06 (-19)	-1.32 ± 0.14 (100.4)
	uLSW	-1.30 ± 0.08	-0.22 ± 0.02 (17)	$-0.01_7 \pm 0.00_1$ (1)	0.25 ± 0.01 (-19)	-1.31 ± 0.08 (101)	-1.09 ± 0.13 (84)	-0.22 ± 0.13 (17)	-1.30 ± 0.08 (100.2)
	cLSW	-1.06 ± 0.08	-0.14 ± 0.04 (13)	$-0.01_6 \pm 0.00_4$ (2)	0.31 ± 0.06 (-29)	-1.22 ± 0.10 (115)	-0.54 ± 0.04 (51)	-0.68 ± 0.11 (64)	-1.07 ± 0.12 (100.4)
	ISOW	-0.82 ± 0.08	0.03 ± 0.02 (-3)	$0.00_4 \pm 0.00_2$ (0)	-0.01 ± 0.05 (1)	-0.85 ± 0.10 (103)	-0.74 ± 0.06 (89)	-0.11 ± 0.07 (14)	-0.83 ± 0.11 (100.4)
	DSOW	-0.91 ± 0.09	-0.06 ± 0.03 (6)	$-0.00_5 \pm 0.00_2$ (1)	0.23 ± 0.06 (-25)	-1.09 ± 0.12 (119)	-0.89 ± 0.08 (97)	-0.20 ± 0.07 (22)	-0.92 ± 0.14 (100.7)
Iceland	SPMW	-1.18 ± 0.09	-0.40 ± 0.08 (34)	-0.03 ± 0.01 (2)	0.44 ± 0.07 (-37)	-1.20 ± 0.11 (102)	-1.25 ± 0.07 (106)	0.05 ± 0.06 (-4)	-1.19 ± 0.15 (100.6)
	uLSW	-0.80 ± 0.05	0.03 ± 0.01 (-4)	$0.00_4 \pm 0.00_1$ (-1)	0.06 ± 0.04 (-7)	-0.90 ± 0.04 (112)	-0.97 ± 0.12 (121)	0.07 ± 0.09 (-9)	-0.81 ± 0.06 (100.4)
	cLSW	-0.76 ± 0.06	0.05 ± 0.02 (-6)	$0.00_7 \pm 0.00_2$ (-1)	0.19 ± 0.05 (-24)	-1.01 ± 0.07 (132)	-0.69 ± 0.05 (91)	-0.31 ± 0.06 (41)	-0.77 ± 0.09 (100.4)
	ISOW	-0.61 ± 0.06	0.03 ± 0.01 (-4)	$0.00_4 \pm 0.00_1$ (-1)	0.31 ± 0.07 (-51)	-0.95 ± 0.08 (156)	-0.54 ± 0.07 (89)	-0.41 ± 0.08 (67)	-0.61 ± 0.10 (100.1)

Biogeosciences Discuss., doi:10.5194/bg-2016-66, 2016
Manuscript under review for journal Biogeosciences
Published: 29 February 2016

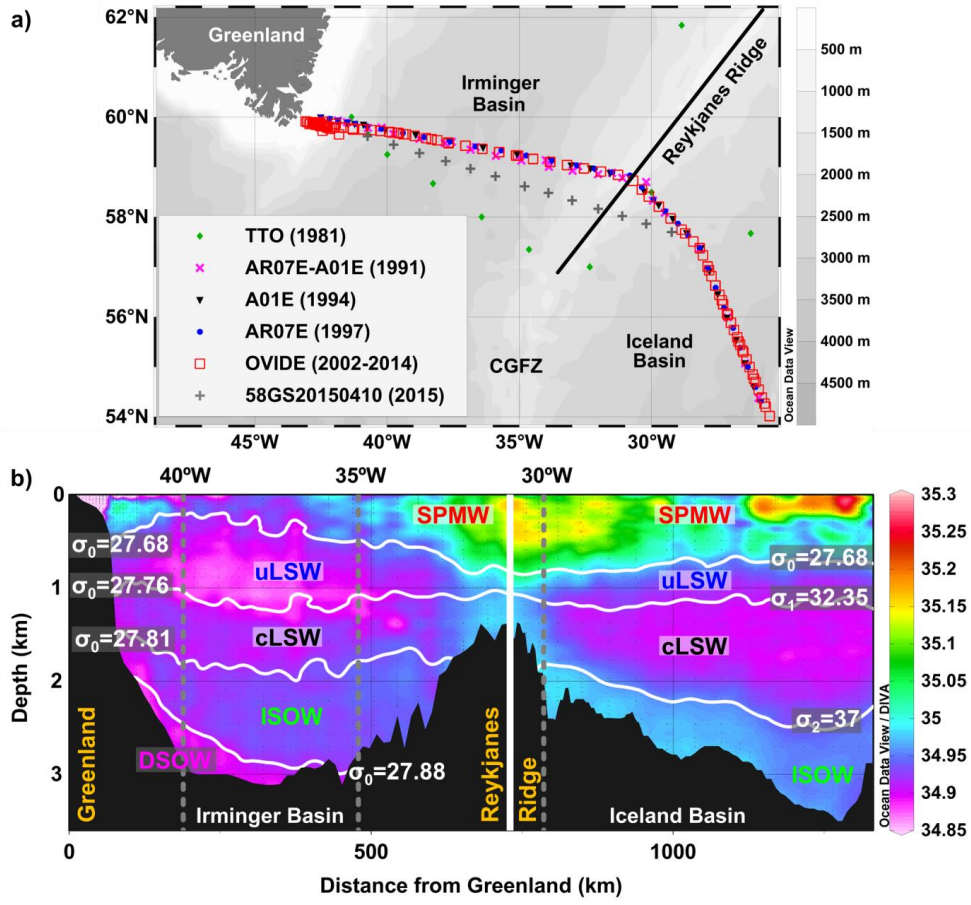

Figure 1: (a) Sampling locations of the thirteen cruises used in this study (1981−2015) plotted on bathymetry (500 m intervals). The black line shows the boundary between the Irminger and the Iceland basins constituted by the Reykjanes Ridge. CGFZ = Charlie−Gibbs Fracture Zone. (b) Limits of the layers and basins considered in this study plotted on top of the mean salinity of the sections. The isopycnals delineating the layers are defined by potential density (σ_0, in kg·m^{-3}), and the vertical white line is the limit (Reykjanes Ridge) between the Irminger (left) and Iceland basins (right). The dashed vertical lines represent the Longitude axis marks. The layer acronyms are Subpolar Mode Water (SPMW), upper and classical Labrador Sea Water (uLSW and cLSW, respectively), Iceland−Scotland Overflow Water (ISOW) and Denmark Strait Overflow Water (DSOW).

Biogeosciences Discuss., doi:10.5194/bg-2016-66, 2016
Manuscript under review for journal Biogeosciences
Published: 29 February 2016

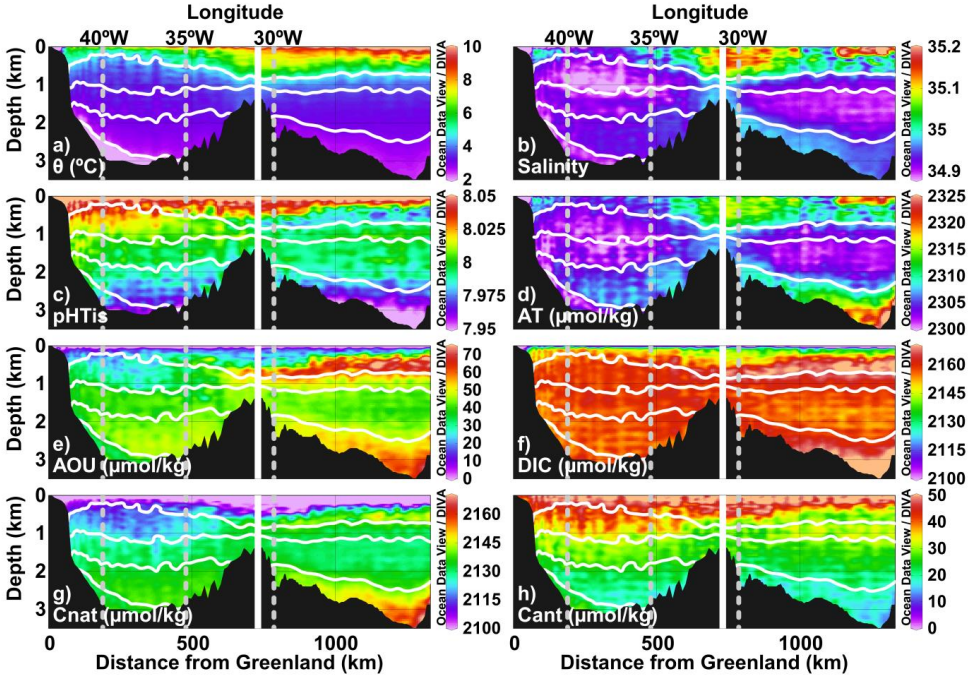

Figure 2: Mean distributions along the cruise track, from Greenland (left) to the Iceland basin (right) over study period (1981−2015), for: (a) potential temperature (θ, in ºC), (b) salinity, (c) pH at total scale and in situ conditions (pHTis), (d) total alkalinity (AT, in µmol·kg^{-1}), (e) apparent oxygen utilization (AOU, in µmol·kg^{-1}), (f) total dissolved inorganic carbon (DIC; in µmol·kg^{-1}), (g) natural DIC (Cnat, in µmol·kg^{-1}) and (h) anthropogenic CO_2 (Cant, in µmol·kg^{-1}). The dashed vertical lines represent the Longitude axis marks.

Biogeosciences Discuss., doi:10.5194/bg-2016-66, 2016
Manuscript under review for journal Biogeosciences
Published: 29 February 2016

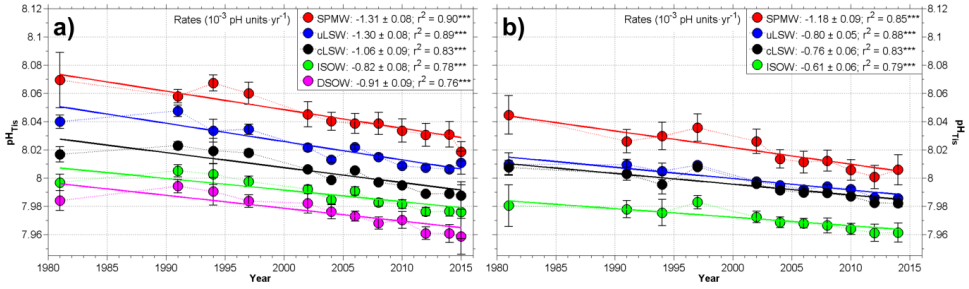

Figure 3: Temporal evolution of average pH at total scale and in situ conditions (pH_{Tis}) in the main water masses of the Irminger (a) and Iceland (b) basins, between 1981 and 2015. Each point represents the average pH_{Tis} of a particular layer (SPMW (red dots), uLSW (blue dots), cLSW (black dots), ISOW (green dots) and DSOW (magenta dots)) at the time of each cruise (Table S1). The error bars are two times the error of the mean (2σ = 2x(Standard Deviation)/$\sqrt{N}$, where N is the number of samples of each layer). The inset boxes give the trends (in 10^{-3} pH units·yr^{-1}) ± standard error of the estimate and the correlation coefficients (r^2), resulting from the annually interpolated values. * denotes that the trend is statistically significant at the 99% level (p-value < 0.01). Confront Fig. 1 for layer acronyms.**

Biogeosciences Discuss., doi:10.5194/bg-2016-66, 2016
Manuscript under review for journal Biogeosciences
Published: 29 February 2016

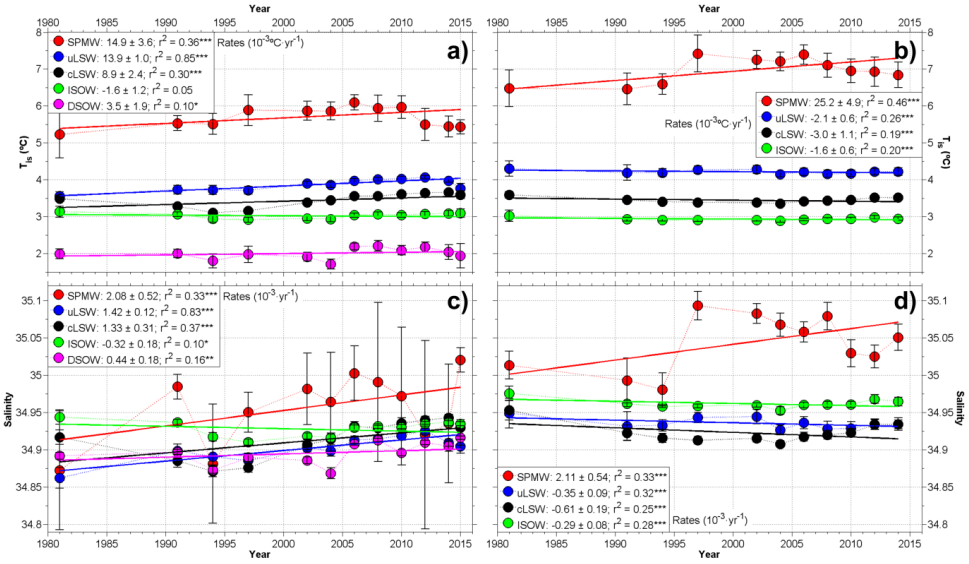

Figure 4: Temporal evolution between 1981 and 2015 of average (a and b) in situ temperature (T_{is}, in ºC) and (c and d) salinity in the main water masses of the Irminger (a and c) and Iceland (b and c) basins. Each point represents the average property of a particular layer (SPMW (red dots), uLSW (blue dots), cLSW (black dots), ISOW (green dots) and DSOW (magenta dots)) at the time of each cruise (Table S1). The error bars are 2σ. The inset boxes give the trends (in 10^{-3} units·yr^{-1}) ± standard error of the estimate and the correlation coefficients (r^2), resulting from the annually interpolated values. * denotes that the trend is statistically significant at the 90% level (p-value < 0.1), ** at the 95% level (p-value < 0.05), and * at 99% level (p-value < 0.01). Confront Fig. 1 for layer acronyms.**

Biogeosciences Discuss., doi:10.5194/bg-2016-66, 2016
Manuscript under review for journal Biogeosciences
Published: 29 February 2016

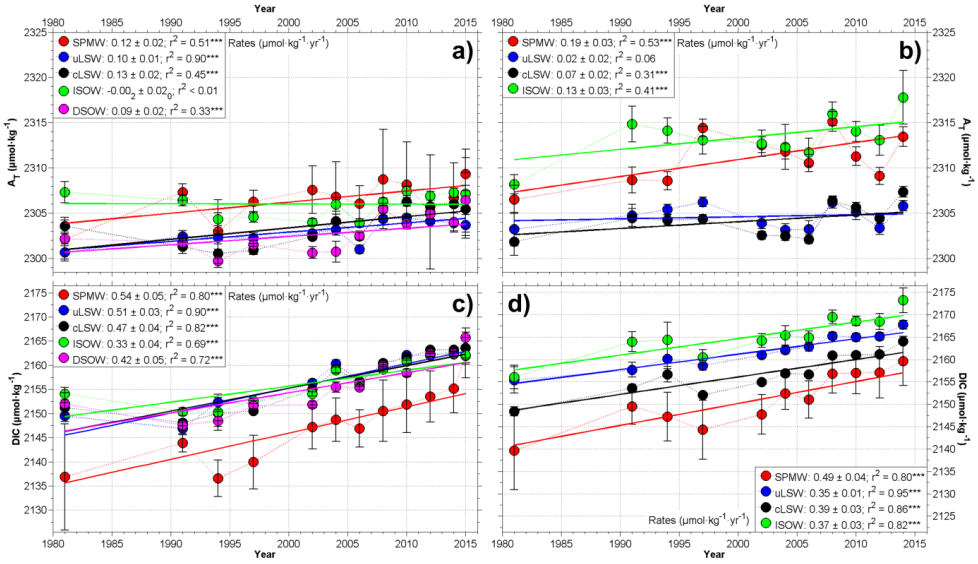

Figure 5: Temporal evolution between 1981 and 2015 of average (a and b) total alkalinity (A_T, in µmol·kg^{-1}) and (c and d) total dissolved inorganic carbon (DIC, in µmol·kg^{-1}) in the main water masses of the Irminger (a and c) and Iceland (b and d) basins. Each point represents the average property of a particular layer (SPMW (red dots), uLSW (blue dots), cLSW (black dots), ISOW (green dots) and DSOW (magenta dots)) at the time of each cruise (Table S1). The error bars are 2σ. The inset boxes give the trends (in µmol·kg^{-1}·yr^{-1}) ± standard error of the estimate and the correlation coefficients (r^2), resulting from the annually interpolated values. * denotes that the trend is statistically significant at the 99% level (p-value < 0.01). Confront Fig. 1 for layer acronyms.**

Biogeosciences Discuss., doi:10.5194/bg-2016-66, 2016
Manuscript under review for journal Biogeosciences
Published: 29 February 2016

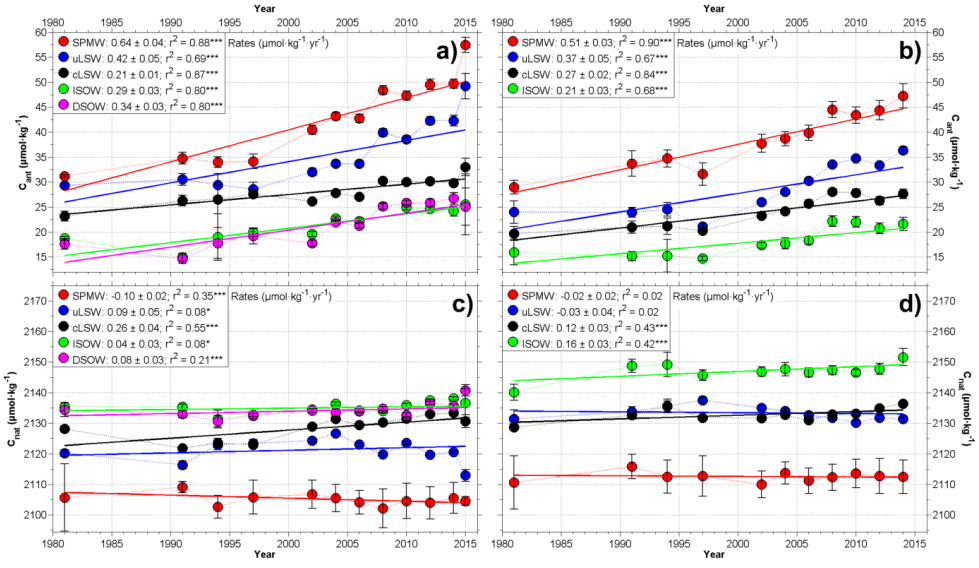

Figure 6: Temporal evolution between 1981 and 2015 of average (a and b) anthropogenic CO_2 (C_{ant}, in µmol·kg^{-1}) and (c and d) natural DIC (C_{nat} = DIC - C_{ant}, in µmol·kg^{-1}) values in the main water masses of the Irminger (a and c) and Iceland (b and c) basins. Each point represents the average property of a particular layer (SPMW (red dots), uLSW (blue dots), cLSW (black dots), ISOW (green dots) and DSOW (magenta dots)) at the time of each cruise (Table S1). The error bars are 2σ. The inset boxes give the trends (in µmol·kg^{-1}·yr^{-1}) ± standard error of the estimate and the correlation coefficients (r^2), resulting from the annually interpolated values. * denotes that the trend is statistically significant at the 90% level (p-value < 0.1), and * at the 99% level (p-value < 0.01). Confront Fig. 1 for layer acronyms.**